Exchange-correlation energy and potential as approximate functionals of occupied and virtual Kohn-Sham orbitals: Application to dissociating H-2

Gruning, M.; Gritsenko, O.V.; Baerends, E.J.

published in
Journal of Chemical Physics
2003

DOI (link to publisher)
10.1063/1.1562197

document version
Publisher's PDF, also known as Version of record

Exchange-correlation energy and potential as approximate functionals of occupied and virtual Kohn–Sham orbitals: Application to dissociating H_2

M. Grüning, O. V. Gritsenko, and E. J. Baerends
Section Theoretical Chemistry, Vrije Universiteit, De Boelelaan 1083, 1081 HV Amsterdam, The Netherlands

(Received 6 December 2002; accepted 29 January 2003)

The standard local density approximation and generalized gradient approximations fail to properly describe the dissociation of an electron pair bond, yielding large errors (on the order of 50 kcal/mol) at long bond distances. To remedy this failure, a self-consistent Kohn–Sham (KS) method is proposed with the exchange-correlation (xc) energy and potential depending on both occupied and virtual KS orbitals. The xc energy functional of Buijse and Baerends [Mol. Phys. **100**, 401 (2002); Phys. Rev. Lett. **87**, 133004 (2001)] is employed, which, based on an ansatz for the xc-hole amplitude, is able to reproduce the important dynamical and nondynamical effects of Coulomb correlation through the efficient use of virtual orbitals. Self-consistent calculations require the corresponding xc potential to be obtained, to which end the optimized effective potential (OEP) method is used within the common energy denominator approximation for the static orbital Green's function. The problem of the asymptotic divergence of the xc potential of the OEP when a finite number of virtual orbitals is used is addressed. The self-consistent calculations reproduce very well the entire H_2 potential curve, describing correctly the gradual buildup of strong left–right correlation in stretched H_2. © *2003 American Institute of Physics.* [DOI: 10.1063/1.1562197]

I. INTRODUCTION

The development of the Kohn–Sham density functional theory (KS DFT) can be viewed as going upstairs the ''Jacob's ladder'' [1] of the exchange-correlation (xc) functionals: from the local density approximation[2] (LDA) to the direct gradient expansion approximation[3,4] (GEA) and generalized gradient approximations[5–8] (GGAs) and then up to the functionals depending on the occupied KS orbitals, such as meta-GGA xc-energy functionals[9–12] and occupied-orbital-dependent exchange[13–16] and xc[17,18] potentials. Recently, DFT has arrived at the level of xc functionals depending on both occupied and virtual KS orbitals.[19,20] Far from being ''art for art's sake,'' this new development is aimed at yet unsolved DFT problems. In particular, in Fig. 1 it is demonstrated that the widely employed LDA and GGA approximations (taking BECKE88–PERDEW86 as an example) fail rather badly in a description of the full potential energy curve for dissociating H_2. The LDA curve exhibits the well-known underestimation of the bond energy close to equilibrium geometry, but it is making a much larger error (ca. 70 kcal/mol) at large distances, although not as large as the restricted Hartree–Fock method (the DFT calculations are also spin and symmetry restricted, since the true Kohn–Sham solutions of this closed-shell system are of that nature and, in fact, exist at all bond distances[21]). The Becke–Perdew (BP) GGA gives the well-known nice correction around the equilibrium geometry. However, while it reduces the error at the dissociation limit compared to the LDA, it still yields a very large error in that case (ca. 45 kcal/mol). The error of the current DFT approximations in the case of electron pair bond dissociation has received less attention than the well-known failure for odd electron systems like H_2^+,[22–24] but is hardly less dramatic. It can easily be seen in Figs. 4 and 5 (to be discussed more extensively in Sec. V) that the GGA error arises since the GGA correlation energy is far too small (not negative enough), an error which is only partly, but by no means sufficiently, compensated by a more negative GGA exchange energy than the exact exchange energy E_x^{KS}. The well-known ''compensation of errors'' between exchange and correlation or, rather, the ''exclusion of nondynamical correlation in the GGA correlation but inclusion into GGA exchange'' [25] breaks down for the extreme nondynamical correlation in the dissociating electron pair bond. It is to be noted that hybrid functionals would not provide a remedy; they would deteriorate the dissociation curve by shifting it towards that of the Hartree–Fock approximation.

As was stressed in Ref. 19, orbital-dependent functionals with inclusion of virtual orbitals seem to be a natural way to describe properly within DFT dissociation of molecular electron pair bonds. It would seem, at first glance, that the functional dependence on virtual orbitals does not present any principal problem. Both occupied and virtual KS orbitals are density functionals $\psi_j(\mathbf{r};[\rho])$, $j \leqslant N/2$; $\psi_a(\mathbf{r};[\rho])$, $a > N/2$ (we consider a closed-shell N electron system), so that the xc energy $E_{\mathrm{xc}}[\rho]$ can be, in principle, considered within the KS energy expression as an orbital-dependent functional:

$$E[\rho] = T_s(\{\psi_j[\rho]\}) + E_{ne}[\rho] + E_H[\rho] + E_{\mathrm{xc}}[\{\psi_j[\rho]\},\{\psi_a[\rho]\}]. \tag{1.1}$$

Other functionals in Eq. (1.1) are the KS kinetic energy T_s, an explicit functional of the occupied orbitals $\{\psi_j\}$, the electron-nuclear attraction energy E_{ne}, and the Hartree en-

ergy of the electrostatic electron repulsion E_H, which are both explicit density functionals of the electron density ρ:

$$\rho(\mathbf{r}_1)=\sum_i n_i|\psi_i(\mathbf{r}_1)|^2, \quad n_i=2,\ i\leqslant N/2; \quad n_i=0,\ i>N/2. \tag{1.2}$$

Within the self-consistent KS theory, the orbitals are determined from the KS one-electron equations

$$\left\{-\frac{1}{2}\nabla^2+v_s(\mathbf{r}_1)\right\}\psi_i(\mathbf{r}_1)=\varepsilon_i\psi_i(\mathbf{r}_1), \tag{1.3}$$

$$v_s(\mathbf{r}_1)=v_{ne}(\mathbf{r}_1)+v_H(\mathbf{r}_1)+v_{\mathrm{xc}}(\mathbf{r}_1), \tag{1.4}$$

where the index i refers to both occupied and virtual orbitals. The local xc potential v_{xc} in Eq. (1.4) can be obtained according to the optimized potential method[26] (OPM) via the chain differentiation rule

$$v_{\mathrm{xc}}(\mathbf{r}_1)=\sum_i \int \frac{\delta E_{\mathrm{xc}}[\{\psi_j\},\{\psi_a\}]}{\delta\psi_i(\mathbf{r}_2)}\frac{\delta\psi_i(\mathbf{r}_2)}{\delta v_s(\mathbf{r}_3)} \times\frac{\delta v_s(\mathbf{r}_3)}{\delta\rho(\mathbf{r}_1)}d\mathbf{r}_2 d\mathbf{r}_3+\text{c.c.} \tag{1.5}$$

from the orbital derivatives of the functional $E_{\mathrm{xc}}[\{\psi_j\},\{\psi_a\}]$. [Sometimes the denotation OPM is used for the exact exchange-only functional, and optimized effective potential (OEP) method for more general orbital-dependent xc functionals.]

Since the exact functional form of E_{xc} is not known, restricted approximate functionals with a finite number M of orbitals are to be taken, so that Eq. (1.5) turns into a finite sum

$$v_{\mathrm{xc}}(\mathbf{r}_1)=\sum_i^M \int \frac{\delta E_{\mathrm{xc}}[\{\psi_j\},\{\psi_a\}]}{\delta\psi_i(\mathbf{r}_2)}\frac{\delta\psi_i(\mathbf{r}_2)}{\delta v_s(\mathbf{r}_3)} \times\frac{\delta v_s(\mathbf{r}_3)}{\delta\rho(\mathbf{r}_1)}d\mathbf{r}_2 d\mathbf{r}_3+\text{c.c.} \tag{1.6}$$

In Ref. 20 a perturbation theoretic approach, yielding the Kohn–Sham analog of the second-order Møller–Plesset (MP2) energy correction, has been used. In Ref. 19 a simple ansatz for $E_{\mathrm{xc}}[\{\psi_j\},\{\psi_a\}]$,[27,28] which can describe strong correlation effects, has been applied to the dissociating H_2 molecule. However, as was recognized in Refs. 19 and 20, the OPM potential v_{xc} of Eq. (1.6) may diverge in the asymptotic region (at long distance) when virtual Kohn–Sham orbitals are included in the xc energy [i.e., $M>N/2$ in Eq. (1.6)], although the Coulombic asymptotics $v_{\mathrm{xc}}(\mathbf{r}_1)\rightarrow -1/|\mathbf{r}_1|$ was established for the exact xc potential.[29]

In this paper an approximate self-consistent KS scheme based on an orbital-dependent xc functional[27,28] is presented. In Sec. II this functional $E_{\mathrm{xc}}[\{\psi_j\},\{\psi_a\}]$ is characterized. The required ''weights'' with which the occupied and virtual orbitals enter, which in the original density-matrix functional formulation were obtained as the square roots of natural orbital occupation numbers, are here written as the square roots of ''fictitious occupations'' $\tilde{n}_i$ that are estimated with a Fermi-type distribution as functions of the orbital energies ε_j. In Sec. III the problem of divergence of the OEP potential (1.6), alluded to above, is considered. It is a consequence of the necessary restriction—in practice—that the number M of the KS orbitals in the functional $E_{\mathrm{xc}}[\{\psi_j\},\{\psi_a\}]$ be finite. In that case the requirement of correct asymptotics of the xc potential should be imposed as a constraint in the optimization of the potential. An appropriate modification of the OEP equations is introduced to achieve correct asymptotics of the constructed v_{xc}. In Sec. IV the OEP equations for the local potential v_{xc} are approximately but accurately and efficiently solved with the recent common energy denominator approximation (CEDA) to the static orbital Green's function.[14,16] In Sec. V an application is made to the prototype electron pair bond, the ground-state potential energy curve of the H_2 molecule. Contrary to the standard LDA and GGA methods, the present method is able to reproduce the whole potential curve of H_2, including the dissociation region. A comparative analysis of individual energy components is made to interpret the obtained results. In Sec. VI implications of the present work for DFT are discussed and the conclusions are drawn.

We note that very recently the problem of dissociation of an electron pair bond, exemplified by the H_2 case, has been approached by many-body perturbation theory based methods, where use of the random phase approximation (RPA) approximation is an essential ingredient.[30–33]

Encouraging results are obtained for the strong nondynamical correlation at long distance, but improvement is still required for the energy at geometries around equilibrium bond length (i.e., atomization energies).

II. (VIRTUAL) ORBITAL-DEPENDENT xc ENERGY FUNCTIONAL

The orbital-dependent functional we will use is obtained with a simple ansatz[27,28] for the density of the xc hole $\bar{\rho}_{\mathrm{xc}}^{\mathrm{hole}}$ which through its potential $\bar{v}_{\mathrm{xc}}^{\mathrm{hole}}$ determines the xc energy,

$$E_{\mathrm{xc}}[\{\psi_j\},\{\psi_a\}]=\frac{1}{2}\int \rho(\mathbf{r}_1)\bar{v}_{\mathrm{xc}}^{\mathrm{hole}}(\mathbf{r}_1)d\mathbf{r}_1 =\frac{1}{2}\int d\mathbf{r}_1\rho(\mathbf{r}_1)\int d\mathbf{r}_2\frac{\bar{\rho}_{\mathrm{xc}}^{\mathrm{hole}}(\mathbf{r}_2|\mathbf{r}_1)}{r_{12}}, \tag{2.1}$$

where the density ρ is the exact density, which can be obtained from the occupied ($n_i=2$) KS orbitals:

$$\rho(\mathbf{r}_1)=\sum_i^{N/2} n_i|\psi_i(\mathbf{r}_1)|^2. \tag{2.2}$$

The overbar in $\bar{\rho}_{\mathrm{xc}}^{\mathrm{hole}}$ and $\bar{v}_{\mathrm{xc}}^{\mathrm{hole}}$ indicates that we are dealing with the coupling-constant integrated xc hole and potential: i.e., the kinetic correlation energy $T-T_s$ is incorporated. In the case of the xc contribution of the electron–electron interaction energy, $W_{\mathrm{xc}}=(1/2)\int\rho(\mathbf{r}_1)v_{\mathrm{xc}}^{\mathrm{hole}}(\mathbf{r}_1)d\mathbf{r}_1=(1/2)\int d\mathbf{r}_1\rho(\mathbf{r}_1)\int d\mathbf{r}_2\rho_{\mathrm{xc}}^{\mathrm{hole}}(\mathbf{r}_2|\mathbf{r}_1)/r_{12}$ ($\rho_{\mathrm{xc}}^{\mathrm{hole}}$ not coupling constant integrated), it has been shown that a very good approximation for the xc hole can be obtained from the ansatz that it is the square of an amplitude $\varphi_{\mathrm{xc}}^{\mathrm{hole}}(\mathbf{r}_2|\mathbf{r}_1)$, $-|\varphi_{\mathrm{xc}}^{\mathrm{hole}}(\mathbf{r}_2|\mathbf{r}_1)|^2=\rho_{\mathrm{xc}}^{\mathrm{hole}}(\mathbf{r}_2|\mathbf{r}_1)$. When the amplitude is expanded in the natural orbitals (NO), the coefficients can be shown, from sym-

metry properties of the two-electron density matrix, to depend on the square roots of the NO occupation numbers.[27,28] The expansion of the hole amplitude into natural orbitals implies that one is approximating the two-electron density matrix in terms of tensor products of the one-electron density matrix. It has been shown by Csanyi and Arias[34] that there is only a limited number of possibilities for such approximate forms, because of the symmetry requirements. A further restriction to one term in the tensor expansion of the two-matrix leads to an approximation which is equivalent to our approximation of the hole as minus the square of an amplitude. These authors indeed also obtain the $\sqrt{n}$ dependence of the coefficients upon expansion in the natural orbitals (cf. Ref. 35 for an earlier argument leading to the same $\sqrt{n}$ dependence). Following Refs. 19 and 28, we propose a similar expression for the amplitude of the coupling constant integrated xc hole, the KS orbitals being used instead of the NOs,

$$\bar{\varphi}_{\mathrm{xc}}^{\mathrm{hole}}(\mathbf{r}_2|\mathbf{r}_1)=\sum_i^M \sqrt{\frac{\tilde{n}_i}{\rho(\mathbf{r}_1)}}\,\psi_i^*(\mathbf{r}_1)\psi_i(\mathbf{r}_2), \tag{2.3}$$

$$\bar{\rho}_{\mathrm{xc}}^{\mathrm{hole}}(\mathbf{r}_2|\mathbf{r}_1)=-\sum_{ij}^M \frac{\sqrt{\tilde{n}_i\tilde{n}_j}}{\rho(\mathbf{r}_1)}\psi_i^*(\mathbf{r}_1)\psi_i(\mathbf{r}_2)\psi_j(\mathbf{r}_1)\psi_j^*(\mathbf{r}_2), \tag{2.4}$$

which yields the orbital-dependent potential of the xc hole $v_{\mathrm{xc}}^{\mathrm{hole}}$,

$$\bar{v}_{\mathrm{xc}}^{\mathrm{hole}}(\mathbf{r}_1)=-\sum_{ij}^M \frac{\sqrt{\tilde{n}_i\tilde{n}_j}}{\rho(\mathbf{r}_1)}\psi_i^*(\mathbf{r}_1)\psi_j(\mathbf{r}_1) \times\int \frac{\psi_i(\mathbf{r}_2)\psi_j^*(\mathbf{r}_2)}{r_{12}}d\mathbf{r}_2, \tag{2.5}$$

and the xc energy functional E_{xc},

$$E_{\mathrm{xc}}[\{\psi_j\},\{\psi_a\}]=-\frac{1}{2}\sum_{ij}^M \sqrt{\tilde{n}_i\tilde{n}_j}\int d\mathbf{r}_1 d\mathbf{r}_2 \times\frac{\psi_i^*(\mathbf{r}_1)\psi_i(\mathbf{r}_2)\psi_j(\mathbf{r}_1)\psi_j^*(\mathbf{r}_2)}{r_{12}}. \tag{2.6}$$

Here the $\tilde{n}_i$ no longer refer to NO occupation numbers, but they are the parameters that govern the involvement of the occupied and virtual KS orbitals in the functional. They have to absorb the change from ''pure'' xc hole to coupling constant integrated hole, and ultimately the success or failure of this functional will depend on our ability to construct a suitable algorithm for the determination of the $\tilde{n}_i$. It should be emphasized that the $\tilde{n}_i$ are *not* the true occupation numbers of the Kohn–Sham orbitals. We continue to use the standard Kohn–Sham prescription of $N/2$ occupied orbitals: i.e., in a closed-shell system, we have Kohn–Sham occupation numbers n_i of either 2.0 or 0.0.

Having been derived in Refs. 27 and 28 as a generalization of the exchange (Fermi) hole amplitude,[36,37] the ansatz (2.3) describes correlation remarkably well for cases of dynamical correlation, such as the He atom [becoming exact in the high-Z two-electron ions with configuration $(1s)^2$] and also for cases of near degeneracy or nondynamical correlation, such as dissociating H_2. In the latter case the Fermi hole ρ_x^{hole} is just minus the density of the σ_g MO, $\rho_x^{\mathrm{hole}}(\mathbf{r}_2|\mathbf{r}_1)=-|\sigma(\mathbf{r}_2)|^2\approx -1/2[|a(\mathbf{r}_2)|^2+|b(\mathbf{r}_2)|^2]$ [a and b are the atomic orbitals (AOs)], so that it does not depend on $\mathbf{r}_1$ and is delocalized over both H atoms. Such delocalization produces the well-known failure of the Hartree–Fock (HF) method for dissociating H_2 (see also Sec. V). Contrary to this, the hole (2.4), which in this case can be fairly represented as

$$\rho_{\mathrm{xc}}^{\mathrm{hole}}(\mathbf{r}_2|\mathbf{r}_1)\approx -\frac{1}{\rho(\mathbf{r}_1)}\{|\sigma_g(\mathbf{r}_1)|^2|\sigma_g(\mathbf{r}_2)|^2 +[\sigma_g^*(\mathbf{r}_1)\sigma_u(\mathbf{r}_1)\sigma_g(\mathbf{r}_2)\sigma_u^*(\mathbf{r}_2)+\mathrm{c.c.}] +|\sigma_u(\mathbf{r}_1)|^2|\sigma_u(\mathbf{r}_2)|^2\}, \tag{2.7}$$

is correctly localized around the reference electron at $\mathbf{r}_1$, i.e., when $\mathbf{r}_1$ is in the neighborhood of atom H_A, $\rho_{\mathrm{xc}}^{\mathrm{hole}}(\mathbf{r}_2|\mathbf{r}_1\in\Omega_A)\approx -|a(\mathbf{r}_2)|^2$. (In this particular case the coupling constant integration has no effect and $\rho_{\mathrm{xc}}^{\mathrm{hole}}$ and $\bar{\rho}_{\mathrm{xc}}^{\mathrm{hole}}$ are identical; see Refs. 19 and 38). This correct form of $\rho_{\mathrm{xc}}^{\mathrm{hole}}$ is the result of the inclusion of the lowest unoccupied molecular orbital (LUMO) σ_u in Eqs. (2.3), (2.4), and (2.7), in particular, through the cross products $\sigma_g^*\sigma_u$ in Eqs. (2.4) and (2.7).

Within the KS scheme (1.1)–(1.7), we consider the fictitious occupations $\tilde{n}_i$ as density functionals and we approximate their functional dependence with the Fermi-type distribution:

$$\tilde{n}_i=\frac{2}{1+\exp[f(\varepsilon_i-\varepsilon_F)]}, \tag{2.8}$$

where ε_i are the KS orbital energies in Eq. (1.3) and the actual form of the model function $f(\varepsilon_i-\varepsilon_F)$ will be considered in Sec. V.

III. OEP DERIVATION OF THE xc POTENTIAL, WITH A CONSTRAINT TO ENSURE PROPER ASYMPTOTIC DECAY

The chain differentiation rule (1.6) for v_{xc} takes into account that all KS orbitals are solutions in the same local KS potential v_s, which is in one-to-one correspondence with the density ρ. It can be easily transformed into the OEP equations, which have originally been formulated explicitly as a variational problem for the energy minimization under variation of the local potential.[26] The second derivative on the right-hand side (RHS) of Eq. (1.6) is expressed through the static orbital Green's function G_i,

$$\frac{\delta\psi_i(\mathbf{r}_2)}{\delta v_s(\mathbf{r}_3)}=-G_i(\mathbf{r}_2,\mathbf{r}_3)\psi_i(\mathbf{r}_3), \tag{3.1}$$

$$G_i(\mathbf{r}_1,\mathbf{r}_2)=\sum_{j\neq i}\frac{\psi_j(\mathbf{r}_1)\psi_j^*(\mathbf{r}_2)}{\varepsilon_j-\varepsilon_i}, \tag{3.2}$$

and the third derivative is the inverse,

$$\frac{\delta v_s(\mathbf{r}_3)}{\delta\rho(\mathbf{r}_1)}=\chi_s^{-1}(\mathbf{r}_3,\mathbf{r}_1), \tag{3.3}$$

of the static KS linear response function χ_s:

$$\chi_s(\mathbf{r}_1,\mathbf{r}_3)=\frac{\delta\rho(\mathbf{r}_1)}{\delta v_s(\mathbf{r}_3)}$$
$$=-\sum_i^{N/2} n_i\psi_i^*(\mathbf{r}_1)G_i(\mathbf{r}_1,\mathbf{r}_3)\psi_i(\mathbf{r}_3)+\text{c.c.},$$
$$n_i=2. \tag{3.4}$$

Inserting Eqs. (3.1) and (3.3) into Eq. (1.6), multiplying both its sides by $\chi_s(\mathbf{r}_1,\mathbf{r}_3)$, integrating over $\mathbf{r}_1$, and relabeling the indices, we obtain the OEP equation

$$\sum_i^{N/2} n_i\psi_i^*(\mathbf{r}_1)\int v_{\text{xc}}(\mathbf{r}_2)G_i(\mathbf{r}_1,\mathbf{r}_2)\psi_i(\mathbf{r}_2)d\mathbf{r}_2+\text{c.c.}$$
$$=\sum_i^M \psi_i^*(\mathbf{r}_1)\int v_{\text{xc}}^i(\mathbf{r}_2)G_i(\mathbf{r}_1,\mathbf{r}_2)\psi_i(\mathbf{r}_2)d\mathbf{r}_2+\text{c.c.}, \tag{3.5}$$

where the nonlocal potentials v_{xc}^k are defined as

$$v_{\text{xc}}^k(\mathbf{r}_2)=\left[\frac{1}{\psi_k(\mathbf{r}_2)}\frac{\delta E_{\text{xc}}[\{\phi_i\}]}{\delta\psi_k^*(\mathbf{r}_2)}\right]. \tag{3.6}$$

According to the analysis of Refs. 20 and 39 it appears that the LHS and RHS of Eq. (3.5) have (as functions of $\mathbf{r}_1$) different asymptotics at $|\mathbf{r}_1|\to\infty$. Indeed, since the Green's function G_i has the asymptotics[20,39,40] $G_i(\mathbf{r}_1,\mathbf{r}_2)\to\psi_i(\mathbf{r}_1)$ at $|\mathbf{r}_1|\gg|\mathbf{r}_2|$, the LHS sum over occupied orbitals decays as the density $|\psi_{N/2}(\mathbf{r}_1)|^2$ of the highest occupied molecular orbital (HOMO) $\psi_{N/2}$. On the other hand, the extended (but still finite) RHS sum decays as the density $|\psi_a(\mathbf{r}_1)|^2$ of the most diffuse virtual orbital ψ_a included in the summation: i.e., it decays more slowly than the LHS. This produces the divergence of the solution of the OEP equations, the potential v_{xc} in the LHS of Eq. (3.5).[20,39] It is to be noted[40] that this divergence is not a necessary consequence of the use of virtual orbitals. If the complete (infinite) set is used, the asymptotic behavior is not necessarily governed by the most diffuse function of the set (which would not be defined anyway in the complete set of KS orbitals which comprises unbound states). The divergence can be considered as the result of the restriction to a finite summation over virtual orbitals in Eq. (1.6) and on the RHS of Eq. (3.5). From a theoretical point of view it is, of course, desirable to operate with a more physically reasonable, nondivergent approximation to v_{xc}. In practice, as was recognized in Refs. 19 and 20, this divergence prevents an approximate solution of the OEP equation (3.5) with virtual KS orbitals with the method of Krieger, Li, Iafrate[13] (KLI) or with the (CEDA).[14,16]

Bearing this in mind, we propose a modification of the OEP equations (1.5) and (3.5), so as to impose correct asymptotic behavior of the xc potential. It has been made clear in Ref. 20 that in the KLI approximation the origin of the divergence can be identified as arising from terms in the potential of the form $\psi_i(\mathbf{r}_1)\psi_j(\mathbf{r}_1)/\rho(\mathbf{r}_1)$. When $\psi_i(\mathbf{r}_1)$ and/or $\psi_j(\mathbf{r}_1)$ are virtual orbitals, the numerator may decay more slowly than the denominator, which asymptotically decays as the highest occupied Kohn–Sham orbital. In the CEDA approximation the same type of terms leads to divergence. As a pragmatic solution, we change the asymptotic behavior of the denominator from $\rho(\mathbf{r})$ to $\tilde{\rho}(\mathbf{r})=\sum_i^M\tilde{n}_i\psi_i(\mathbf{r})^*\psi_i(\mathbf{r})$: i.e., we interpret the fictitious occupation numbers $\tilde{n}_i$ in the xc functional as effective occupation numbers in an effective density $\tilde{\rho}(\mathbf{r})$, which is only used in the denominator of expressions we derive according to the KLI or CEDA approximation for the potential (see below). It is to be expected that $\tilde{\rho}(\mathbf{r})$ is actually a close approximation to $\rho(\mathbf{r})$, except for the crucial difference in how these two densities tend asymptotically to zero. That this is the case can be easily verified in the case of dissociating H_2, which wil be discussed in Sec. V.

IV. EXPLICIT EXPRESSION FOR v_{xc} USING THE CEDA TO THE OEP METHOD

We now proceed to the derivation of v_{xc} corresponding to the (virtual) orbital-dependent xc functional of Sec. II by the common energy denominator approximation.[14,16] The CEDA approximation uses for the static orbital Green's function G_i,

$$G_i^{\text{CEDA}}(\mathbf{r}_1,\mathbf{r}_2)\approx\frac{\delta(\mathbf{r}_1-\mathbf{r}_2)}{\Delta\varepsilon}-\frac{1}{\Delta\varepsilon}\sum_j^M \psi_j(\mathbf{r}_1)\psi_j^*(\mathbf{r}_2)$$
$$+\sum_{j\neq i}^M\frac{\psi_j(\mathbf{r}_1)\psi_j^*(\mathbf{r}_2)}{\varepsilon_j-\varepsilon_i}=\frac{\delta(\mathbf{r}_1-\mathbf{r}_2)}{\Delta\varepsilon}$$
$$-\frac{1}{\Delta\varepsilon}\sum_j^M d_{ij}\psi_j(\mathbf{r}_1)\psi_j^*(\mathbf{r}_2), \tag{4.1}$$

where $d_{ij}=[\varepsilon_j-\varepsilon_i-\Delta\varepsilon(1-\delta_{ij})]/(\varepsilon_j-\varepsilon_i)]$, i.e., $d_{ij}=1$ when $i=j$ and $d_{ij}=1-\Delta\varepsilon/(\varepsilon_j-\varepsilon_i)$ when $i\neq j$. This Green's function includes all occupied KS orbitals ψ_i, $i\leqslant N/2$, and some unoccupied ones ψ_a, $N/2<a\leqslant M$, in finite summations. The third term in the first line of Eq. (4.1) is the rigorous expression for G_i truncated to M orbitals, while the first and second terms with a common energy denominator $\Delta\varepsilon$ produce an estimate of the remaining terms.

To get an explicit expression for the potential v_{xc} in terms of the occupied and virtual orbitals, we insert the CEDA Green's function (4.1) in the OEP equation (3.5), thus obtaining the equation for the v_{xc} potential:

$$\frac{1}{\Delta\varepsilon}\sum_i^{N/2} n_i v_{\text{xc}}^{\text{CEDA}}(\mathbf{r}_1)|\psi_i(\mathbf{r}_1)|^2-\frac{1}{\Delta\varepsilon}\sum_i^M v_{\text{xc}}^i(\mathbf{r}_1)|\psi_i(\mathbf{r}_1)|^2$$
$$-\frac{1}{\Delta\varepsilon}\sum_i^{N/2}\sum_j^M d_{ij}n_i v_{\text{xc},ji}^{\text{CEDA}}\psi_i^*(\mathbf{r}_1)\psi_j(\mathbf{r}_1)$$
$$+\frac{1}{\Delta\varepsilon}\sum_i^M\sum_j^M d_{ij}v_{\text{xc},ji}^i\psi_i^*(\mathbf{r}_1)\psi_j(\mathbf{r}_1)+\text{c.c.}=0, \tag{4.2}$$

where v_{xc}^i is the orbital derivative of the xc energy functional (2.6),

$$v_{\text{xc}}^i(\mathbf{r}_1)=\frac{1}{\psi_i(\mathbf{r}_1)}\frac{\delta E_{\text{xc}}}{\delta\psi_i^*(\mathbf{r}_1)}$$
$$=-\sum_j^M\sqrt{\tilde{n}_i\tilde{n}_j}\frac{\psi_j(\mathbf{r}_1)}{\psi_i(\mathbf{r}_1)}\int\frac{\psi_i(\mathbf{r}_2)\psi_j^*(\mathbf{r}_2)}{r_{12}}d\mathbf{r}_2, \tag{4.3}$$

and $v_{\text{xc},ji}^{\text{CEDA}}$, and $v_{\text{xc},ji}^i$ are the matrix elements of the potentials $v_{\text{xc}}^{\text{CEDA}}$ and v_{xc}^i for the orbitals ψ_j^* and ψ_i:

$$v_{\mathrm{xc},ji}^{\mathrm{CEDA}}=\int \psi_j^*(\mathbf{r}_2)v_{\mathrm{xc}}^{\mathrm{CEDA}}(\mathbf{r}_2)\psi_i(\mathbf{r}_2)d\mathbf{r}_2, \tag{4.4}$$

$$v_{\mathrm{xc},ji}^{i}=\int \psi_j^*(\mathbf{r}_2)v_{\mathrm{xc}}^{i}(\mathbf{r}_2)\psi_i(\mathbf{r}_2)d\mathbf{r}_2. \tag{4.5}$$

From Eq. (4.2) it follows that

$$v_{\mathrm{xc}}^{\mathrm{CEDA}}(\mathbf{r}_1)=\bar{v}_{\mathrm{xc}}^{\mathrm{hole}}(\mathbf{r}_1)+\sum_i^{N/2}\sum_j^{M} d_{ij}n_i \times \mathrm{Re}[v_{\mathrm{xc},ji}^{\mathrm{CEDA}}\psi_i^*(\mathbf{r}_1)\psi_j(\mathbf{r}_1)]\frac{1}{\rho(\mathbf{r}_1)} -\sum_i^{M}\sum_j^{M} d_{ij}\,\mathrm{Re}[v_{\mathrm{xc},ji}^{i}\psi_i^*(\mathbf{r}_1)\psi_j(\mathbf{r}_1)]\frac{1}{\rho(\mathbf{r}_1)}, \tag{4.6}$$

where $\bar{v}_{\mathrm{xc}}^{\mathrm{hole}}(\mathbf{r}_1)$ is the xc-hole potential (2.5):

$$\bar{v}_{\mathrm{xc}}^{\mathrm{hole}}(\mathbf{r}_1)=\sum_i^{M}\frac{|\psi_i(\mathbf{r}_1)|^2\,\mathrm{Re}[v_{\mathrm{xc}}^{i}(\mathbf{r}_1)]}{\rho(\mathbf{r}_1)}. \tag{4.7}$$

Note that divergence of the potentials (4.7) and (4.6) is avoided by replacing the asymptotic behavior of $\rho(\mathbf{r})$ in terms with diffuse orbital products in the numerator with that of $\tilde{\rho}(\mathbf{r})$, which is, as discussed earlier, the way in which we introduce the constraint that the potential should not diverge. This comment is also applicable to subsequent equations like Eq. (4.8), etc., and will not be repeated.

In the following we will, for simplicity of notation, specialize to real orbitals, which is the case at hand. Equation (4.6) can be solved in the same way as the corresponding equations for the potential of KLI (Ref. 13) or the occupied-orbital-dependent CEDA potential,[14,16,41]

$$v_{\mathrm{xc}}^{\mathrm{CEDA}}(\mathbf{r}_1)=\bar{v}_{\mathrm{xc}}^{\mathrm{hole}}(\mathbf{r}_1)+\sum_i^{N/2}\sum_j^{M} d_{ij}n_i v_{\mathrm{xc},ij}^{\mathrm{CEDA}}\frac{\psi_i(\mathbf{r}_1)\psi_j(\mathbf{r}_1)}{\rho(\mathbf{r}_1)} -\sum_i^{N/2}\sum_j^{M} d_{ij}v_{\mathrm{xc},ij}^{i}\frac{\psi_i(\mathbf{r}_1)\psi_j(\mathbf{r}_1)}{\rho(\mathbf{r}_1)}. \tag{4.8}$$

Multiplying both sides of Eq. (4.8) by $\psi_k(\mathbf{r}_1)\psi_l(\mathbf{r}_1)$ ($k\leqslant N/2$, $l\leqslant M$) and integrating over $\mathbf{r}_1$, one obtains the equations for the matrix elements $v_{\mathrm{xc},ij}^{\mathrm{CEDA}}$,

$$\sum_i^{N/2}\sum_j^{M}(\delta_{ki}\delta_{lj}-M_{kl,ij})v_{\mathrm{xc},ij}^{\mathrm{CEDA}}=\bar{v}_{\mathrm{xc},kl}^{\mathrm{hole}}-\sum_i^{M}\sum_j^{M}N_{kl,ij}v_{\mathrm{xc},ij}^{i}, \tag{4.9}$$

where $M_{kl,ij}$ and $N_{kl,ij}$ are the weighted overlap integrals between the orbital products $\psi_k\psi_l$ and $\psi_i\psi_j$,

$$M_{kl,ij}=n_i d_{ij}\int\frac{\psi_k(\mathbf{r}_1)\psi_l(\mathbf{r}_1)\psi_i(\mathbf{r}_1)\psi_j(\mathbf{r}_1)}{\rho(\mathbf{r}_1)}d\mathbf{r}_1,$$

$$N_{kl,ij}=M_{kl,ij}/n_i, \tag{4.10}$$

and $\bar{v}_{\mathrm{xc},kl}^{\mathrm{hole}}$ is the matrix element of the xc-hole potential (4.7),

$$\bar{v}_{\mathrm{xc},kl}^{\mathrm{hole}}=\sum_i^{M}\int\frac{\psi_k(\mathbf{r}_1)\psi_l(\mathbf{r}_1)\psi_i^2(\mathbf{r}_1)v_{\mathrm{xc}}^{i}(\mathbf{r}_1)}{\rho(\mathbf{r}_1)}d\mathbf{r}_1. \tag{4.11}$$

Equations (4.9) for the constants $v_{\mathrm{xc},ij}^{\mathrm{CEDA}}$ are, like the KLI equations are for the KLI constants, a dependent set of linear equations. In fact, it is easily verified that the $N/2$ rows with $k=l$ are linearly dependent (multiplying these rows with n_k and summing them leads to a row of zeros, and the right-hand side becomes zero as well). We therefore can only solve for $M\cdot N/2-1$ unknowns and have chosen $v_{\mathrm{xc},N/2N/2}^{\mathrm{CEDA}}$ as the undetermined constant that can be chosen freely. It has been conveniently put to zero. So Eq. (4.9) is solved by inversion of the square subblock $(\mathbf{I}-\mathbf{M})'$ of the matrix $(\mathbf{I}-\mathbf{M})$, where $1\leqslant i,\ k\leqslant N/2$ and $1\leqslant j,\ l\leqslant M$), but with $i=j=N/2$ and $k=l=N/2$ excluded (rows are indexed with kl and columns with ij) Defining the $M\cdot N/2-1$ by the $M\cdot N/2-1$ matrix ξ and the $M\cdot N/2-1$ by the $M\cdot N/2$ matrix η,

$$\xi_{mn,kl}=[(\mathbf{I}-\mathbf{M})']^{-1}_{mn,kl}, \tag{4.12a}$$

with rows $\xi_{N/2\,N/2,mn}$ and columns $\xi_{mn,N/2\,N/2}$ nonexistent,

$$\eta_{mn,ij}=\sum_k^{N/2\,\prime}\sum_l^{M\,\prime}\xi_{mn,kl}N_{kl,ij}, \tag{4.12b}$$

where the primes on the summations mean omission of the $k=l=N/2$ term, we obtain, upon multiplying Eq. (4.9) with $\xi_{mn,kl}$ and summing over kl,

$$v_{\mathrm{xc},mn}^{\mathrm{CEDA}}=\sum_k^{N/2\,\prime}\sum_l^{M\,\prime}\xi_{mn,kl}\bar{v}_{\mathrm{xc},kl}^{\mathrm{hole}}-\sum_i^{M}\sum_j^{M}\eta_{mn,ij}v_{\mathrm{xc},ij}^{i}. \tag{4.13}$$

Finally, inserting Eq. (4.13) into Eq. (4.8), we obtain for $v_{\mathrm{xc}}^{\mathrm{CEDA}}$ the expression

$$v_{\mathrm{xc}}^{\mathrm{CEDA}}(\mathbf{r}_1)=\bar{v}_{\mathrm{xc}}^{\mathrm{hole}}(\mathbf{r}_1)+v_{\mathrm{resp}}^{\mathrm{CEDA}}(\mathbf{r}_1), \tag{4.14}$$

where $v_{\mathrm{resp}}^{\mathrm{CEDA}}$ is the response potential,

$$v_{\mathrm{resp}}^{\mathrm{CEDA}}(\mathbf{r}_1)=\sum_{i,j}^{M}w_{ij}\frac{\psi_i(\mathbf{r}_1)\psi_j(\mathbf{r}_1)}{\tilde{\rho}(\mathbf{r}_1)}, \tag{4.15}$$

where for $\theta(k)=1$ for $k\geqslant 0$ and $\theta(k)=0$ for $k<0$,

$$w_{ij}=\theta\left(\frac{N}{2}-i\right)d_{ij}n_i v_{\mathrm{xc},ij}^{\mathrm{CEDA}}-d_{ij}v_{\mathrm{xc},ij}^{i}\quad(v_{\mathrm{xc},N/2\,N/2}^{\mathrm{CEDA}}=0). \tag{4.16}$$

With our choice of $v_{\mathrm{xc},N/2\,N/2}^{\mathrm{CEDA}}=0$, the potential does not asymptotically go to zero, but to a constant. However, we have found that the inversion of $(\mathbf{I}-\mathbf{M})'$ may become numerically less stable when a $v_{\mathrm{xc},ia}^{\mathrm{CEDA}}$ related to a diffuse orbital ψ_a with low effective occupation $\tilde{n}_a$ is chosen as the free constant. The constant asymptotic behavior has no consequences: if desired, a shift can be applied to the total potential to make it asymptotically tend to zero. Equations (4.7) and (4.14)–(4.16) define the Kohn–Sham xc potential $v_{\mathrm{xc}}^{\mathrm{CEDA}}$ corresponding within the modified OPM-CEDA to the orbital-dependent xc energy functional (2.6). Here $v_{\mathrm{xc}}^{\mathrm{CEDA}}$ is subdivided naturally into an attractive xc-hole potential $\bar{v}_{\mathrm{xc}}^{\mathrm{hole}}(\mathbf{r}_1)$ and a repulsive response potential $v_{\mathrm{resp}}^{\mathrm{CEDA}}(\mathbf{r}_1)$. The former potential represents the main exchange-correlation effect, namely, the interaction of the reference electron with the xc hole in the distribution of other electrons. In particular, due to the inclusion of virtual KS orbitals, the present $\bar{v}_{\mathrm{xc}}^{\mathrm{hole}}(\mathbf{r}_1)$ represents the important effects of Coulomb corre-

lation discussed in Sec. II. By construction, the present $\bar{v}_{\rm xc}^{\rm hole}(\mathbf{r}_1)$ has Coulombic long-range asymptotics $\bar{v}_{\rm xc}^{\rm hole}(\mathbf{r}_1) \rightarrow -1/|\mathbf{r}_1|$ at $|\mathbf{r}_1| \rightarrow \infty$.

In turn, the response potential $v_{\rm resp}^{\rm CEDA}$ of Eq. (4.15) has the characteristic orbital step structure with the step heights w_{ij} of Eq. (4.16) corresponding to the individual orbital products $\psi_i\psi_j$ in Eq. (4.15). The orbital structure follows from the fact that in the region, where a particular orbital density ψ_i^2 brings a dominant contribution to the effective density $\tilde{\rho}$, the potential $v_{\rm resp}^{\rm CEDA}$ is close to the corresponding weight w_{ii}. The form of the present response part of the xc potential, $v_{\rm resp}^{\rm CEDA}$ of Eq. (4.15), is similar to that of the KLI (Ref. 13) or CEDA (Refs. 14 and 16) exchange-only response potentials and the correlation manifests itself in the presence of ''steps'' with products ψ_a^2 and $\psi_a\psi_j$ of virtual orbitals ψ_a.

V. CALCULATION OF THE H_2 POTENTIAL CURVE

Based on the theory presented in the previous sections, we propose a self-consistent KS scheme with our occupied and virtual orbital-dependent xc energy functional. In this scheme the total energy is

$$E = T_s[\{n_i\},\{\psi_i\}] + E_{ne}[\rho(\mathbf{r})] + E_H[\rho] + E_{\rm xc}[\{\tilde{n}_i\},\{\psi_i\}], \tag{5.1}$$

where $E_{\rm xc}$ is defined with Eq. (2.6). The orbitals ψ_i in Eq. (5.1) are obtained from the KS one-electron equations

$$\left\{ -\frac{1}{2}\nabla^2 + v_{ne}(\mathbf{r}_1) + v_H(\mathbf{r}_1) + v_{\rm xc}^{\rm CEDA}(\mathbf{r}_1) \right\} \psi_i(\mathbf{r}_1) = \varepsilon_i \psi_i(\mathbf{r}_1), \tag{5.2}$$

where $v_{\rm xc}^{\rm CEDA}$ is defined with Eqs. (4.7) and (4.14)–(4.18). The functionals T_s, E_{ne}, and E_H in Eq. (5.1) and the potential v_H in Eq. (5.2) are calculated with the conventional KS density (1.2), i.e., with the occupations n_i of the orbitals ψ_i, while the expressions for $E_{\rm xc}$ and $v_{\rm xc}^{\rm CEDA}$ contain the fictitious occupations $\tilde{n}_i$. The latter are calculated within the self-consistent procedure as explicit functions (2.8) of the orbital energies. In this paper we use the Fermi-type distribution

$$\tilde{n}_i = \frac{2}{1+\exp[(\varepsilon_i-\varepsilon_F)/\sqrt{a(\varepsilon_{(N/2+1)}-\varepsilon_{N/2})+b(\varepsilon_{(N/2+1)}-\varepsilon_{N/2})^2}]}, \tag{5.3}$$

with the parameters a and b, which appears to be flexible enough for our purpose. In Eq. (5.3), $\varepsilon_{N/2}$ and $\varepsilon_{(N/2+1)}$ are the HOMO and LUMO energies. The parameter ε_F is determined to satisfy the normalization condition $\Sigma_i^M \tilde{n}_i = N$, which yields a value close to $(\varepsilon_{\rm LUMO}+\varepsilon_{\rm HOMO})/2$ for ε_F. Alternatively, one can fix ε_F at the average of HOMO and LUMO energies and scale the $\tilde{n}_i$ so that $\Sigma_i^M \tilde{n}_i = N$ is satisfied. These procedures both work well.

We apply the self-consistent method of Eqs. (5.1)–(5.3) to the calculation of the potential curve of the H_2 molecule. The nine lowest virtual orbitals have been included in the summations in the xc energy (2.6) and the xc potential $v_{\rm xc}^{\rm CEDA}$. Figure 1 compares the total energy curve obtained with the xc energy functional (2.6) (denoted BB) with those calculated with the HF and full configuration interaction (FCI) methods as well as with the LDA and with a GGA consisting of a combination (BP) of Becke's[7] exchange (B88) and Perdew's[5] (P86) correlation functionals. The correlation-consistent triple-zeta basis cc-pVTZ (Ref. 42), of Gaussian-type orbitals (GTOs) has been used. All calculations have been performed within the spin-restricted approach by means of a Gaussian orbital density functional code[27,43] based on the ATMOL package.[44]

Figure 1 clearly displays the failures of HF, LDA, and GGA-BP for the H_2 potential curve. The most dramatic is the well-known HF failure due to the neglect of the Coulomb correlation in the HF method. The HF curve goes higher than other curves at nearly all the H–H distances and at R(H–H) = 10 bohrs the error of the HF total energy, $E^{\rm HF} - E^{\rm FCI} = 148$ kcal/mol, and the error of the dissociation energy [estimated at R(H–H) = 10 bohrs and comparing to $E(R_e)$], $D_e^{\rm HF} - D_e^{\rm FCI} = 123$ kcal/mol. The displayed failure of the LDA and standard GGA is, perhaps, less well known than their poor performance for the dissociating cation H_2^+,[22–24] the total energy of which the GGAs greatly underestimate (ca. 60 kcal/mol too negative). In contrast, the spin-restricted LDA and GGA-BP greatly overestimate the energy of the dissociating H_2 (see Fig. 1), although not as much as HF. In particular, near the equilibrium distance R(H–H) = 1.401 bohr the LDA curve is close to the HF one, while at large R(H–H) it goes in between the HF and FCI curves. At R(H–H) = 10 bohrs the LDA total energy error $E^{\rm LDA} - E^{\rm FCI} = 69$ kcal/mol and the LDA dissociation energy error $D_e^{\rm LDA} - D_e^{\rm FCI} = 46$ kcal/mol. The gradient correction lowers the GGA-BP energy compared to the LDA one, and the BP curve goes below and almost in parallel to the LDA curve. Near equilibrium the BP curve is close to the FCI one: however, BP still considerably overestimates the energy at long distance. The BP total energy error at R(H–H) = 10 bohrs is $E^{\rm BP} - E^{\rm FCI} = 44$ kcal/mol, and the BP dissociation energy error $D_e^{\rm BP} - D_e^{\rm FCI} = 47$ kcal/mol is even slightly larger than the LDA one.

The errors in the DFT dissociation energies seem to contradict the notion that the LDA and GGA approximations, by the very fact that they work with model holes that are local, do not exhibit the typical Hartree–Fock error due to the com-

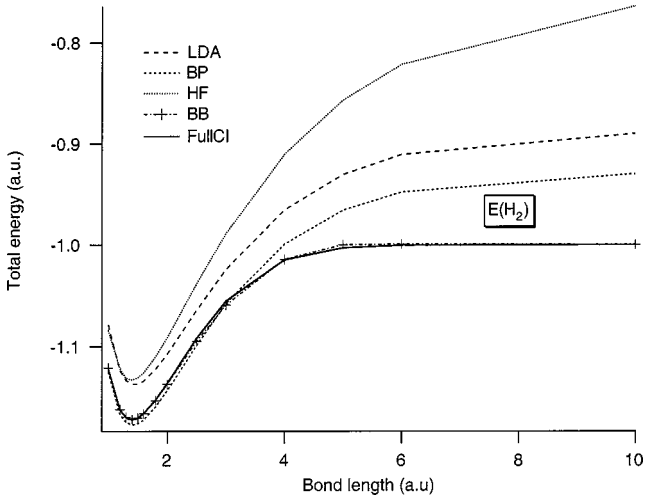

FIG. 1. Total energy of H_2 as a function of internuclear distance for the Hartree–Fock approximation (HF), the local-density approximation (LDA), the BECKE88–PERDEW86 generalized gradient approximation (BP), a full–CI calculation, and the exchange-correlation functional of Refs. 19 and 28 (BB).

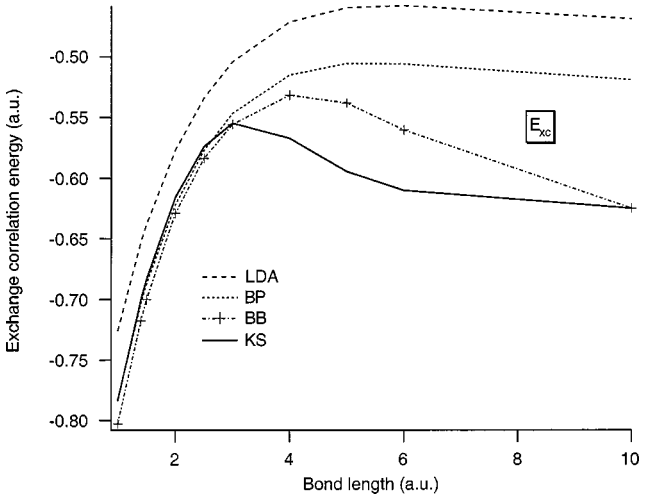

FIG. 2. Total exchange-correlation energy for the exact Kohn–Sham model (KS) and for various approximate exchange-correlation functionals; see caption of Fig. 1.

pletely delocalized exchange hole. Apparently the local nature of the holes of the LDA and GGA approximations is not sufficient to ensure proper behavior at long distance, a point to which we will return below.

In contrast to the LDA and GGA curves, the potential curve of the self-consistent BB method (5.1)–(5.3) excellently reproduces the FCI curve: both curves practically coincide at all H–H distances (see Fig. 1). The best agreement is achieved for the parameters $a=0.008$ and $b=0.045$ in the distribution (5.3) with a total energy average error (for various H–H distances) of only -0.07 kcal/mol, an average absolute error of 0.72 kcal/mol, and a maximal error of -2.4 kcal/mol at $R(\mathrm{H–H})=3$ bohrs. The important feature of the functional (2.6) is its correct behavior for dissociating H_2 (see Sec. II). Due to this, the dissociation energy error is only -0.20 kcal/mol.

The above-mentioned energy differences of the LDA, GGA and BB, which share the same functionals T_s, E_{ne}, and E_H, originate from the different xc functionals of these methods. Figure 2 compares their $E_{\mathrm{xc}}(R)$ curves with the benchmark curve $E_{\mathrm{xc}}^{\mathrm{KS}}(R)$ for the accurate KS solution obtained from the FCI density ρ_{FCI} with the iterative scheme of van Leeuwen and Baerends.[45] One can see from Fig. 2, that the LDA and GGA-BP xc energies as functions of $R(\mathrm{H–H})$ have a qualitatively different behavior compared to the accurate $E_{\mathrm{xc}}^{\mathrm{KS}}$. Both LDA and BP xc energies increase monotonically with $R(\mathrm{H–H})$, with the latter being consistently lower than the former. In its turn, $E_{\mathrm{xc}}^{\mathrm{KS}}[R(\mathrm{H–H})]$ passes through a maximum at $R(\mathrm{H–H})=3$ bohrs and at larger $R(\mathrm{H–H})$ it decreases monotonically. For the distances $R(\mathrm{H–H})\leqslant 3$ bohrs the GGA energy $E_{\mathrm{xc}}^{\mathrm{BP}}$ is close to $E_{\mathrm{xc}}^{\mathrm{KS}}$: however, both the LDA and BP greatly overestimate the xc energy of dissociating H_2 (i.e., do not have it negative enough). The corresponding errors at $R(\mathrm{H–H})=10$ bohrs of 98 and 66 kcal/mol are, in fact, larger than the abovementioned LDA-GGA total energy errors. Thus the latter errors originate from the errors of the LDA-GGA xc functionals, which are partly compensated with the errors of opposite sign in other energy components.

Contrary to the LDA and GGA, the BB xc functional (2.6) reproduces qualitatively the benchmark dependence $E_{\mathrm{xc}}^{\mathrm{KS}}(R)$ (see Fig. 2). $E_{\mathrm{xc}}^{\mathrm{BB}}$ is close to $E_{\mathrm{xc}}^{\mathrm{KS}}$ for $R(\mathrm{H–H})\leqslant 3$ bohrs, and it again coincides with $E_{\mathrm{xc}}^{\mathrm{KS}}$ at large $R(\mathrm{H–H})$. Note, however, that the maximum of the BB curve is somewhat displaced from that of $E_{\mathrm{xc}}^{\mathrm{KS}}(R)$ and $E_{\mathrm{xc}}^{\mathrm{BB}}$ differs appreciably from $E_{\mathrm{xc}}^{\mathrm{KS}}$ in the region $3.5\leqslant R(\mathrm{H–H})\leqslant 8$ bohrs. This indicates that the very good BB total energies in this region (see Fig. 1) are the result of compensation of errors of opposite signs in various energy components.

This compensation can be clearly seen when one compares Fig. 2 with Fig. 3: the latter figure presents the dependence of the LDA, BP, BB, and KS kinetic energies T_s and the HF kinetic energy T^{HF} on $R(\mathrm{H–H})$. While the $E_{\mathrm{xc}}^{\mathrm{BB}}$ energy is higher than $E_{\mathrm{xc}}^{\mathrm{KS}}$ in the region $3.5\leqslant R(\mathrm{H–H})\leqslant 8$ bohrs (see Fig. 2), the BB kinetic energy T_s^{BB} is lower

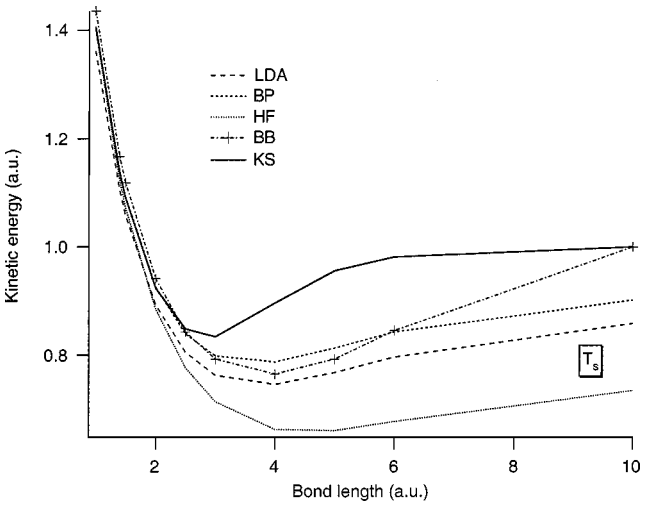

FIG. 3. Kohn–Sham kinetic energy T_s for H_2 as a function of internuclear distance for the exact Kohn–Sham model (KS) and for calculations with various approximate exchange-correlation functionals; see caption of Fig. 1.

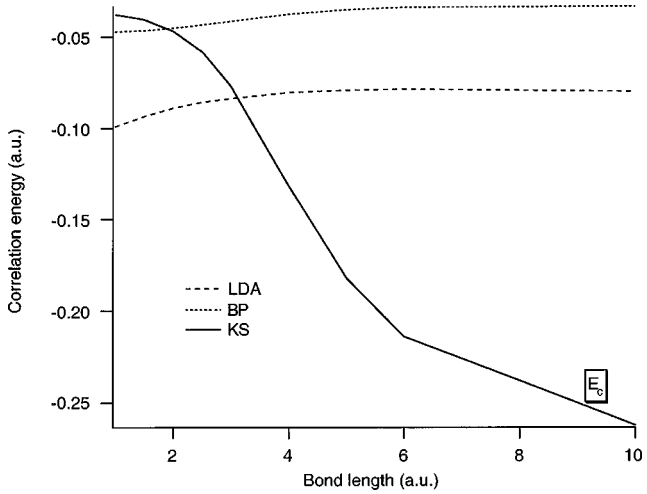

FIG. 4. Correlation energy for H_2 as a function of internuclear distance for the exact Kohn–Sham model (KS) and the LDA and GGA-BP approximations.

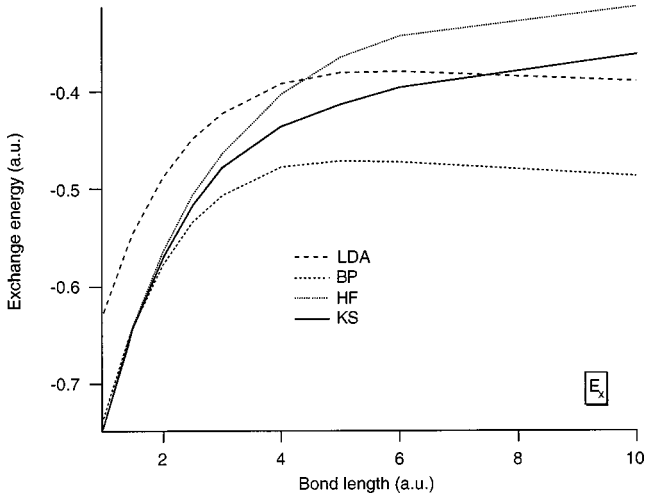

FIG. 5. Exchange energy for H_2 as a function of internuclear distance for Hartree–Fock (HF), the exact Kohn–Sham model (KS), and the LDA and GGA-BP approximations.

than T_s^{KS} in the same region (see Fig. 3). Note that in the case of H_2 only the lowest MO σ_g contributes to T_s and T^{HF}, so that comparison of the kinetic energies reveals the relative size of the σ_g MO in various methods: the more diffuse σ_g is in a particular method, the lower is T_s. Thus Fig. 3 indicates a well-known feature of the HF approximation: a too diffuse character of the HF σ_g MO for dissociating H_2. Indeed, for larger R(H–H) the HF kinetic curve goes much lower than other curves. Judging from this criterion, the LDA yields a more contracted (towards the nuclei) σ_g than the HF approximation; the GGA-BP further increases this contraction and in BB the size of σ_g gradually changes with R(H–H) from that of BP to that of σ_g of the accurate KS solution.

Further analysis shows that the above-mentioned underestimation of the xc energy of dissociating H_2 (in the sense of being not negative enough) by the LDA and GGA is due to the inability of these methods to grasp nondynamical left–right electron correlation in the stretched H_2 molecule. Figure 4 displays the totally different dependence on R(H–H) of the LDA–GGA correlation energy functionals and the benchmark correlation energy E_c^{KS} corresponding to the accurate KS solution. The S-shaped $E_c^{\mathrm{KS}}(R)$ curve represents a rather sharp transition from dynamical-like correlation in the region R(H–H)$=1.4-2.5$ bohrs to strong nondynamical correlation for R(H–H)>7 bohrs. Indeed, near equilibrium E_c^{KS} is close to the typical energy -0.045 hartree of the dynamical correlation of an electron pair in atomic systems. On the other hand, due to the strong left–right correlation at larger R(H–H), E_c^{KS} exceeds -0.25 hartree at R(H–H)$=10$ bohrs; i.e., it experiences a 4.5-fold increase in its absolute value.

In its turn, the LDA–GGA correlation energy remains nearly constant for all R(H–H), with E_c^{LDA} being about twice as low as the GGA E_c^P (see Fig. 4). This happens because the LDA functional represents Coulomb correlation in a model system, the homogeneous electron gas,[2] for which the correlation energy per particle $\varepsilon_c(\rho)$ at typical atomic electron densities ρ is about twice that of dynamical electron correlation in atoms. The gradient correction of GGA-P86 removes this discrepancy and near the equilibrium E_c^P is close to E_c^{KS}. Still both the LDA and P86 share the basic shallow logarithmic dependence of $\varepsilon_c[\rho(\mathbf{r}_1)]$ on the local density $\rho(\mathbf{r}_1)$, to which a dependence on the local density gradient $\nabla\rho(\mathbf{r}_1)$ is added in P86. With this local $\rho(\mathbf{r}_1)$ dependence, the LDA and GGA have no way to describe, from the H atom densities with which a zero correlation energy corresponds in the isolated atoms, the above-mentioned buildup of the strong left–right nondynamical correlation, which is a characteristic feature of dissociating H_2.

Indeed, according to the interpretation of the GGA performance given in Refs. 25, 46, and 47, in typical cases of covalent bonds nondynamical correlation should be effectively taken into account not by the GGA correlation functionals, but by the GGA exchange functionals. This proved to be almost quantitatively the case for the molecules N_2, Li_2, and F_2, at their equilibrium geometries, as discussed in Ref. 25. We therefore expect GGA exchange energies that are more negative than the HF or KS exchange energy by the nondynamical correlation energy. Figure 5 compares, along the H_2 dissociation coordinate, the B88 exchange energy with the HF one as well as with the energy E_x^{KS} corresponding to the accurate KS solution. Let us first comment on the difference between HF and KS exchange energies. We note that around R_e the HF and KS exchange energies are very similar. For long H–H distances, however, the KS exchange energy becomes clearly lower than the HF exchange energy. Usually, the KS and HF exchange energies are quite close,[25] being little affected by the small differences between HF and KS orbitals. In the present case, however, the HF density and the HF σ_g orbital are significantly too diffuse,[48] and the KS exchange energy, which is based on the more contracted true density [the exchange hole is $-(1/2)\rho$] becomes clearly more negative. Let us next compare the DFT exchange energies (LDA and GGA-BP) to the "true" exchange energy E_x^{KS}. At long distance the LDA and in particular the GGA exchange energy indeed become significantly more negative than E_x^{KS}, in agreement with the notion that it incorporates nondynami-

cal correlation, i.e., has effectively a more localized hole than the true, delocalized, exchange hole. However, the GGA exchange energy at 10 bohrs is only ca. 80 kcal/mol more negative than E_x^{KS}, but from Fig. 4 it is clear that it should have been some 146 kcal/mol more negative in order to cover the very large error in the GGA correlation energy with respect to the full correlation energy. As a consequence, the total GGA exchange-correlation energy of Fig. 2 is not nearly negative enough. So the observation that the GGA exchange energy incorporates the nondynamical correlation energy almost quantitatively at equilibrium geometry[25] does not extend to the more extreme case of nondynamical correlation in the dissociating electron pair bond.

It appears that the general notion that the LDA and GGA are superior for dissociating H_2, and for weak electron-pair bonds in general, due to the inherent locality of the ''exchange'' hole which mimics the full, local, exchange-correlation hole, is not wrong (the dissociation curves in Fig. 1 are indeed much better for the LDA and GGA than for the HF approximation), but is not quantitatively reliable. This can be easily understood from the fact that the DFT exchange holes are not deep and localized enough. Let us consider the full exchange-correlation hole $\rho_{\mathrm{xc}}^{\mathrm{hole}}(\mathbf{r}_2|\mathbf{r}_1)$, which is a function of position coordinate $\mathbf{r}_2$ and surrounds a reference position $\mathbf{r}_1$ that is in the neighborhood of one H nucleus. It has a depth $\rho_{\mathrm{xc}}^{\mathrm{hole}}(\mathbf{r}_1|\mathbf{r}_1)=-\rho(\mathbf{r}_1)$ at $\mathbf{r}_1$ and in fact its shape is $-\rho(\mathbf{r}_2)$ at the H atom where the reference position $\mathbf{r}_1$ is located (and zero at the other H atom): cf. Refs. 19 and 48. The exchange-correlation hole integrates to -1 electron, and so does the exchange hole. The exchange hole, however, has a depth of only $-(1/2)\rho(\mathbf{r}_1)$ since it is only in the electronic density of either spin-α or spin-β electrons. We can roughly estimate the effect of the difference in depth between the complete exchange-correlation hole and exchange-only hole. When one uses the simple Slater model that the hole has uniform depth [either $-\rho(\mathbf{r}_1)$ for $\rho_{\mathrm{xc}}^{\mathrm{hole}}(\mathbf{r}_2|\mathbf{r}_1)$ or $-(1/2)\rho(\mathbf{r}_1)$ for $\rho_x^{\mathrm{hole}}(\mathbf{r}_1|\mathbf{r}_1)$] and radius R such that it integrates to -1 electron, then one obtains for the xc energy

$$E_{\mathrm{xc}}^{\mathrm{model}}=-\frac{1}{2}\int d\mathbf{r}_1\rho(\mathbf{r}_1)\int d\mathbf{r}_2\frac{\rho_{\mathrm{xc}}^{\mathrm{hole}}(\mathbf{r}_2|\mathbf{r}_1)}{r_{12}}$$

$$\approx-\frac{4\pi}{2}\int d\mathbf{r}_1\rho^2(\mathbf{r}_1)\int_0^R r_{12}dr_{12}, \tag{5.4}$$

the simple estimate

$$E_{\mathrm{xc}}^{\mathrm{model}}\approx-\left(\frac{9\pi}{16}\right)^{1/3}\int\rho^{4/3}(\mathbf{r}_1)d\mathbf{r}_1. \tag{5.5}$$

The radius $R=\{3/[4\pi\rho(\mathbf{r}_1)]\}^{1/3}$ is here taken from the unit sum rule. This is 1.27 times as large in absolute magnitude as the exchange energy obtained with a uniform hole of depth $-(1/2)\rho(\mathbf{r}_1)$:

$$E_x^{\mathrm{model}}\approx-\left(\frac{9\pi}{32}\right)^{1/3}\int\rho^{4/3}(\mathbf{r}_1)d\mathbf{r}_1. \tag{5.6}$$

This is roughly comparable to the ratio of $E_{\mathrm{xc}}^{\mathrm{KS}}$ (see Fig. 2) and $E_{\mathrm{xc}}^{\mathrm{BP}}$ (see Fig. 5) $E_{\mathrm{xc}}^{\mathrm{KS}}/E_{\mathrm{xc}}^{\mathrm{BP}}=1.21$ at $R(\mathrm{H–H})=10$ bohrs. This supports the view that the breakdown of the DFT exchange hole models for the description of the nondynamical correlation in this case is a simple consequence of their shallowness. The large difference with a hole that is not only ''localized'' (on one H-atom site), but also of sufficient depth can be compensated neither with the B88 exchange gradient correction nor with the addition of relatively small LDA–GGA correlation energies (see Fig. 4), so that a dramatic underestimation results of the xc (see Fig. 2) and total (see Fig. 1) energies of dissociating H_2 with the LDA and GGA-BP. It is to be noted that hybrid functionals, which introduce a more delocalized hole than the LDA or GGA, would do worse than the pure density functionals at long distance.

Note that, based on the concept of the xc hole, the functional of Eq. (2.6) treats exchange and correlation in a unified way, so that the $E_{\mathrm{xc}}^{\mathrm{BB}}$ curve (Fig. 2) cannot be separated in exchange (Fig. 5) and correlation (Fig. 4) curves, as can be done for LDA and GGA approximations. Still, comparison of the total BB and FCI energies (see Fig. 1) and the xc BB and KS energies (see Fig. 2) shows that due to the proper modelling of the xc hole with inclusion of virtual orbitals, the BB functional reproduces successfully the buildup of strong nondynamical left–right correlation in dissociating H_2.

VI. CONCLUSIONS

In this paper the functional dependence on virtual Kohn–Sham orbitals has been incorporated into the self-consistent KS method. To accomplish this, several methodological questions had to be addressed and solved.

Foremost among them is the choice of an exchange-correlation energy functional, which would efficiently utilize both occupied and virtual orbitals. In this paper the functional proposed by Buijse and Baerends[27,28] has been employed. With its simple orbital dependence (2.6) derived from an ansatz for the xc-hole amplitude, $E_{\mathrm{xc}}^{\mathrm{BB}}$ is able to reproduce the important dynamical and nondynamical effects of Coulomb correlation through the efficient use of virtual orbitals.

The next question to be addressed is the construction of the Kohn–Sham potential, which now also depends on both occupied and virtual orbitals. The problem here is the asymptotical divergence of the xc potential, since it depends on a finite number of the KS orbitals. The problem is evident from the construction of the potential by functional differentiation or, equivalently, by the OEP scheme. In order to build in the desirable constraint of correct (finite) asymptotic behavior, a modification of the OEP equations has been proposed, which leads to a finite xc potential. With a generalization of the common energy denominator approximation for the static orbital Green's function, the explicit expression in terms of occupied and virtual orbitals has been derived for the xc potential $v_{\mathrm{xc}}^{\mathrm{CEDA\text{-}BB}}$ corresponding to the $E_{\mathrm{xc}}^{\mathrm{BB}}$ functional.

The present method requires an algorithm for the involvement (''weight'') of the virtual KS orbitals in the xc functional. In this paper this has been realized by using the analogy with the development of one-electron density matrix dependent xc part of the two-electron density matrix, which

leads to a $\sqrt{n_i}$ dependence (where n_i are the natural orbital occupation numbers) in the coefficients for the expansion of the xc hole in terms of natural orbitals.[27,28,34,35,49] We have used weights in the form of $\sqrt{\tilde{n}_i}$, where $\tilde{n}_i$ are fictitious "occupation numbers" which were approximated with a Fermi-type distribution dependence on the orbital energies.

The resulting self-consistent method has been applied to calculation of the H_2 potential curve and a detailed comparison has been made with HF, FCI, LDA, and GGA-BP methods as well as with the energy components corresponding to the accurate KS solution for H_2. The failure of spin-restricted LDA and GGA-BP has been stressed: the LDA and GGA greatly underestimate the bond energy and the xc energy of dissociating H_2, due to their inability to grasp the strong left–right electron correlation at large H–H distances.

In its turn, the present method reproduces very well the entire H_2 potential curve and it reproduces qualitatively (but not quantitatively) the dependence of the xc energy on the H–H distance. With the proper inclusion of virtual KS orbitals in its orbital structure the functional (2.6) correctly describes the transition from a dynamical-like correlation near the equlibrium to the strong left–right correlation in stretched H_2. Of particular importance is the correct asymptotic behavior of the functional at large R(H–H). In this region the localized xc hole that is implicit in this functional[19] correctly describes the combined effect of exchange and left–right correlation, so that the total energy and its components coincide with the corresponding FCI and accurate KS quantities.

These results demonstrate, in principle, the ability of a functional like $E_{\mathrm{xc}}^{\mathrm{BB}}$ with virtual orbital dependence to describe properly dissociation of molecular electron pair bonds. This is especially encouraging, since the observed failure of the LDA and BP-GGA demonstrates the virtual impossibility of functionals that use only local information (local density and derivatives of the density) to represent the gradual buildup of the strong nondynamical correlation which accompanies bond dissociation. Such nonlocal information is built into the $E_{\mathrm{xc}}^{\mathrm{BB}}$ functional through its orbital dependence, which makes it a full fledged (not only perturbatively defined) exchange *plus* correlation functional.

Nevertheless, important problems remain to be solved. Further development of functionals along these lines will depend on finding a successful scheme to determine the effective weights of the occupied and virtual orbitals or, equivalently, the fictitious "occupations" $\tilde{n}_i$. The present Fermi-type distribution (2.8) and (5.3) can be considered as only a provisional answer. In the second place the problem of the asymptotic divergence of the Kohn–Sham potential arising from the use of a finite set of virtual orbitals has only been addressed in an *ad hoc* manner in this paper.

ACKNOWLEDGMENT

The authors wish to thank Dr. Robert van Leeuwen for early contributions and for enlightening discussions.

[1] J. P. Perdew, in DFT 2000, Satellite Symposium of the 10th International Congress of Quantum Chemistry, Menton, France, 2000.
[2] *Theory of the Inhomogeneous Electron Gas*, edited by S. Lundqvist and N. H. March (Plenum, New York, 1983).
[3] F. Herman, J. P. van Dyke, and I. B. Ortenburger, Phys. Rev. Lett. **22**, 807 (1969).
[4] F. Herman, I. B. Ortenburger, and J. P. van Dyke, Int. J. Quantum Chem., Symp. **3**, 827 (1970).
[5] J. P. Perdew, Phys. Rev. B **33**, 8822 (1986); **34**, 7406 (1986).
[6] C. Lee, W. Yang, and R. G. Parr, Phys. Rev. B **37**, 785 (1988).
[7] A. Becke, Phys. Rev. A **38**, 3098 (1988).
[8] J. P. Perdew, K. Burke, and Y. Wang, Phys. Rev. B **54**, 16533 (1996).
[9] E. I. Proynov, S. D. Sirois, and D. R. Salahub, Int. J. Quantum Chem. **64**, 427 (1997).
[10] M. Filatov and W. Thiel, Chem. Phys. Lett. **295**, 467 (1998).
[11] T. van Voorhis and G. E. Scuseria, J. Chem. Phys. **109**, 400 (1998).
[12] J. P. Perdew, S. Kurth, A. Zupan, and P. Blaha, Phys. Rev. Lett. **82**, 2544 (1999).
[13] J. B. Krieger, Y. Li, and G. J. Iafrate, Phys. Rev. A **45**, 101 (1992).
[14] O. V. Gritsenko and E. J. Baerends, Phys. Rev. A **64**, 042506 (2001).
[15] F. Della Sala and A. Görling, J. Chem. Phys. **115**, 5718 (2001).
[16] M. Grüning, O. V. Gritsenko, and E. J. Baerends, J. Chem. Phys. **116**, 6435 (2002).
[17] P. R. T. Schipper, O. V. Gritsenko, S. J. A. van Gisbergen, and E. J. Baerends, J. Chem. Phys. **112**, 1344 (2000).
[18] M. Grüning, O. V. Gritsenko, S. J. A. van Gisbergen, and E. J. Baerends, J. Chem. Phys. **116**, 9591 (2002).
[19] E. J. Baerends, Phys. Rev. Lett. **87**, 133004 (2001).
[20] A. Facco Bonetti, E. Engel, R. N. Schmid, and R. M. Dreizler, Phys. Rev. Lett. **86**, 2241 (2001).
[21] O. V. Gritsenko and E. J. Baerends, Theor. Chem. Acc. **96**, 44 (1997).
[22] T. Bally and G. N. Sastry, J. Phys. Chem. A **101**, 7923 (1997).
[23] B. Braida, P. C. Hiberty, and A. Savin, J. Phys. Chem. A **102**, 7872 (1998).
[24] M. Sodupe, J. Bertran, L. Rodriguez-Santiago, and E. J. Baerends, J. Phys. Chem. A **103**, 166 (1998).
[25] O. V. Gritsenko, P. R. T. Schipper, and E. J. Baerends, J. Chem. Phys. **107**, 5007 (1997).
[26] J. D. Talman and W. F. Shadwick, Phys. Rev. A **14**, 36 (1976).
[27] M. A. Buijse, Ph.D. thesis, Vrije Universiteit, 1991.
[28] M. A. Buijse and E. J. Baerends, Mol. Phys. **100**, 401 (2002).
[29] C. O. Almbladh and U. von Barth, Phys. Rev. B **31**, 3231 (1985).
[30] F. Furche, Phys. Rev. B **64**, 195120 (2001).
[31] M. Fuchs and X. Gonze, Phys. Rev. B **65**, 235109 (2002).
[32] M. Fuchs, Y. M. Niquet, and X. Gonze (unpublished).
[33] F. Aryasetiawan, T. Miyake, and K. Terakura, Phys. Rev. Lett. **88**, 166401 (2002).
[34] G. Csanyi and T. A. Arias, Phys. Rev. B **61**, 7348 (2000).
[35] A. M. K. Müller, Phys. Lett. **105A**, 446 (1984).
[36] W. L. Luken and D. N. Beratan, Theor. Chim. Acta **61**, 265 (1982).
[37] W. L. Luken, Int. J. Quantum Chem. **22**, 889 (1982).
[38] O. V. Gritsenko, R. van Leeuwen, and E. J. Baerends, Int. J. Quantum Chem. **60**, 1375 (1996).
[39] E. Engel, A. Facco Bonetti, S. Keller, I. Andrejkovics, and R. M. Dreizler, Phys. Rev. A **58**, 964 (1998).
[40] R. van Leeuwen (personal communication).
[41] R. van Leeuwen, O. V. Gritsenko, and E. J. Baerends, Z. Phys. D: At., Mol. Clusters **33**, 229 (1995).
[42] D. E. Woon and T. H. Dunning, J. Chem. Phys. **103**, 4572 (1995).
[43] M. A. Buijse, E. J. Baerends, and J. G. Snijders, Phys. Rev. A **40**, 4190 (1989).
[44] V. R. Saunders and J. H. van Lenthe, Mol. Phys. **48**, 923 (1983).
[45] R. van Leeuwen and E. J. Baerends, Phys. Rev. A **49**, 2421 (1994).
[46] P. R. T. Schipper, O. V. Gritsenko, and E. J. Baerends, Phys. Rev. A **57**, 1729 (1998).
[47] O. V. Gritsenko, B. Ensing, P. R. T. Schipper, and E. J. Baerends, J. Phys. Chem. A **104**, 8558 (2000).
[48] E. J. Baerends and O. V. Gritsenko, J. Phys. Chem. A **101**, 5383 (1997).
[49] S. Goedecker and C. J. Umrigar, Phys. Rev. Lett. **81**, 866 (1998).